Dietary palmitic acid induces trained immunity that controls inflammation and infection

Seufert AL[1], Traxler SK[1], Hickman JW[1], Peterson RM[1], Lashley SJ[2], Shulzhenko N[3], Napier RJ[2,4], and Napier BA[1,*]

Author Affiliations: [1]Department of Biology and Center for Life in Extreme Environments, Portland State University, Portland, OR, 97201, [2]VA Portland Health Care System, Portland, OR, 97239, [3]Department of Biomedical Sciences, Oregon State University, Corvallis, OR, [4]Department of Molecular Microbiology and Immunology, Oregon Health & Sciences University, Portland, OR, 97239, United States.

*Corresponding Author: Dr. Brooke A Napier

Robertson Life Sciences Building

6th Floor Rm 6N087

Portland, OR 97201

E-mail address: brnapier@pdx.edu

ABSTRACT

Trained immunity is epigenetic reprogramming that occurs in innate immune cells in response to primary inflammatory stimuli and leads to enhanced inflammation upon secondary challenge with homologous or heterologous stimuli. We find exposure to high-fat diets confers a hyper-inflammatory response to systemic LPS and enhanced mortality, independent of microbiome. Ketogenic diet (KD) does not alter homeostatic inflammation, but enhances the response of immune cells to LPS challenge *ex vivo*. Lipidomics identified dietary palmitic acid (C16:0; PA) may be acting as a primary inflammatory stimulus in our model. Here we show PA induces a hyper-inflammatory response to LPS challenge in cultured macrophages and *in vivo*, correlating with increased endotoxemia mortality and enhanced resistance to *C. albicans* infection in $RAG^{-/-}$ mice. Our study identifies PA is an inducer of trained immunity that leads to a hyper-inflammatory response to secondary heterologous stimuli, and is deleterious during systemic inflammation, but enhances resistance to infection.

INTRODUCTION

Recent publications have highlighted the regulatory capacity of high-fat diets (HFDs) in driving functional reprogramming of in innate immune cells and inflammatory disease outcome (*1-4*). Specifically, our group has previously reported the Western Diet (WD), a diet high in sugars and saturated fatty acids (SFAs) and low in fiber, leads to increased chronic inflammation (metaflammation) and functional reprogramming of monocyte and neutrophil populations. Moreover, we showed WD-fed mice exhibited increased lipopolysaccharide (LPS)-driven endotoxemia severity and associated-immunoparalysis (*1*). These WD-dependent disease phenotypes were independent of microbiome and diet-associated weight gain, suggesting that these disease phenotypes were due to dietary constituents.

Here, we build on these results by showing chronic exposure to the Ketogenic Diet (KD), a diet exclusively enriched in SFAs and low in carbohydrates, confers an increase in LPS-induced endotoxemia severity and mortality (Fig 1). These results are consistent with previous findings showing that short-exposure to KD is correlated with an increase in endotoxemia mortality (*5*) and that WD increases systemic inflammatory cytokine secretion and NLRP3 activation in atherosclerotic mice treated with LPS (*2*). We add to these studies, by finding these results are independent of glycolytic shock, nutritional ketosis, and the KD-dependent

microbiome (Fig S1; Fig 2). Further, we find KD drives enhanced inflammatory cytokine expression in *ex vivo* monocytes and splenocytes challenged with LPS (Fig 3), suggesting the KD diet induces functional reprogramming in immune cells that allow for an enhanced response to secondary stimuli.

In an effort to identify target immunomodulatory SFAs within a HFD, we defined the lipid profiles of KD mice and found KD-fed mice have significantly altered circulating lipid profiles. Specifically, KD-fed mice show an enrichment of palmitic acid (C16:0; PA) and PA-associated lipids in the blood of KD-fed mice (Fig 4). PA is a SFA found in animal fats, coconut and palm oils, and it is enriched in both the WD and KD. Mechanistically, we define PA and a similar SFA, pentadecanoic acid (C15:0; PDA), as acute inducers of a hyper-inflammatory response in primary macrophages challenged with LPS (Fig 5). These data agree with previous studies showing that PA induces increased transcription of inflammatory cytokines in response to challenge with LPS in human monocytes (*6-8*).Together, these data suggest PA may be inducing “non-antigen specific innate immune memory” in cells of monocyte lineage. Specifically, trained immunity is a type of “non-antigen specific innate immune memory”, and is the concept that a primary inflammatory stimulus (ex: microbial ligand, Bacillus Calmette-Guérin (BCG) vaccine, etc.) induces epigenetic reprogramming of innate immune cells resulting in a quicker, stronger response against a heterologous inflammatory stimulus. This innate immune memory can last up to months in humans and mice (*8*), and likely evolved to provide non-specific protection from secondary infections. However, an enhanced immune response to a secondary stimulus can be deleterious in the context of inflammatory disease or chronic inflammation (*9, 10*). Importantly, we found that shorter (12h) and longer (9 day) exposure to PA is sufficient to drive long-lasting trained immunity in response to systemic LPS, and increased resistance to systemic fungal infection independent of mature lymphocytes.

These are the first results to identify a specific dietary fatty acid as an inducer of trained immunity, and compliment previous findings that show raw bovine milk and host-derived oxidized low-density lipoprotein (oxLDL) particles can induce non-antigen specific innate memory responses within human monocytes and macrophages (*11-13*). Together, these results highlight the importance of identifying host dietary factors that manipulate the inflammatory response to microbial products, and the impact of immunomodulation in the context of a society that is heavily dependent on diets enriched in SFAs. Further, these data identified a PA-induced inflammatory process that can be potentially targeted to modulate or reverse detrimental immune programming by chronic exposure to diets enriched in SFAs.

RESULTS

Diets enriched in saturated fatty acids increase endotoxemia severity and mortality

We have previously found that mice fed Western Diet (WD) showed increased disease severity and mortality in a model of endotoxemia, independent of the WD-dependent microbiome or associated weight gain (*1*). Considering the WD is enriched in dietary saturated fatty acids (SFAs), which have been shown to enhance production of inflammatory cytokines from innate immune cells *in vitro* (*14-17*). Thus, we sought to understand if enriched dietary SFAs were sufficient to drive enhanced endotoxemia severity and mortality *in vivo*.

To examine the immune effects of chronic exposure to diets enriched in SFAs on endotoxemia, we fed mice either a WD (enriched in SFAs and sucrose), a ketogenic diet (KD; enriched in SFAs and low-carbohydrate), or standard chow (SC; low in SFAs and sucrose), for 2 weeks (wk) prior to endotoxemia induction (Table S1). We defined 2 wk of feeding as chronic exposure, because this is correlated with WD- or KD-dependent microbiome changes, and confers metaflammation in WD mice (*1*), sustained altered blood glucose levels (Fig S1A), and elevated levels of the ketones Acetoacetate (AcAc) (Fig S1B) in the urine and *β*-hydroxybutyrate (BHB) in the blood of KD-fed mice (Fig S1C) (*18*). We then induced endotoxemia by a single intraperitoneal (i.p.) injection of LPS in order to induce pathophysiology that resembles symptoms of acute septic shock in humans, including systemic arterial hypotension and increased circulating levels of TNF and IL-6 (*19*). We measured temperature loss, or hypothermia, as a measure of disease severity and survival to determine outcome (*1, 20, 21*). WD- and KD-fed mice showed significant and prolonged hypothermia, starting at 10 hours (h) post-injection (p.i.), compared to the SC-fed mice that experienced mild and transient hypothermia (Fig 1A). In accordance with these findings, WD- and KD-fed mice displayed 100% mortality by 26 h p.i. compared to 100% survival of SC-fed mice (Fig 1B). LPS-induced hypoglycemia is a known driver of endotoxemia mortality, and each of these diets has varying levels of sugars and carbohydrates (Table S1) (*22, 23*). However, mice in all diet groups displayed similar levels of hypoglycemia during disease (Fig S1D), indicating that potential effects of diet on blood glucose were not a driver of enhanced endotoxemia severity.

Mice fed KD experience a shift towards nutritional ketosis, a metabolic state regulated by the liver when blood glucose levels are low. During ketosis endogenous and exogenous FAs are used to synthesize the

ketone bodies acetoacetate, β-hydroxybutyrate, and acetate, which are then distributed to other tissues for energy (*24*). Thus, we wanted to understand if our phenotype was dependent on nutritional ketosis. Thus, mice were fed for 2 wk (chronic exposure) with KD, SC supplemented with saccharine and 1,3-butanediol (SC + BD), a compound that induces ketosis independent of diet (*18*), or SC-fed with the saccharine vehicle solution as a control (SC + Veh). Next, we induced endotoxemia and found KD-fed mice showed significantly greater temperature loss, and a significant survival defect compared to SC + BD-fed (SC + BD), and SC + Veh-fed mice (SC + Veh) (Fig S1E, F). Though not significant when compared to SC + Veh, the SC + BD mice did confer an increase in hypothermia and decrease in survival suggesting that nutritional ketosis may play a minor role in KD-dependent susceptibility to LPS lethality (Fig S1E, F). Together these data suggest that diets enriched in SFAs promote enhanced endotoxemia severity and this is independent of diet-dependent hypoglycemic shock or nutritional ketosis.

Diets enriched in SFAs induce a hyper-inflammatory response to LPS and increased immunoparalysis

Endotoxemia mortality results exclusively from a systemic inflammatory response, characterized by an acute increase in circulating inflammatory cytokine levels (ex: TNF, IL-6, and IL-1β) from splenocytes and myeloid derived innate immune cells (monocytes and macrophages) (*5, 25-27*). Pre-treatment of monocytes and macrophages with dietary SFAs has been shown to enhance inflammatory pathways in response to microbial ligands, including IL-1β and TNF expression and protein levels (*15, 28, 29*). Considering this, we hypothesized that exposure to enriched dietary SFAs within the WD and KD would enhance the inflammatory response to systemic LPS during endotoxemia. Thus, we induced endotoxemia and measured the differences in the systemic inflammatory response via expression of inflammatory cytokines in the blood (*tnf*, *il-6*, and *il-1β*) every 5 h from 0 - 20 h p.i. At 5 h p.i., mice fed all diets showed induction of *tnf, il-6*, and *il-1β* expression in the blood (Fig 1C-E). However, WD- and KD-fed mice experienced significantly higher expression of *tnf, il-6*, and *il-1β* in the blood at 5 h p.i., compared with SC-fed mice (Fig 1C-E), indicating that diets enriched in SFAs are associated with a hyper-inflammatory response to LPS.

Sepsis patients often present with two immune phases: an initial amplification of inflammation, followed-by or concurrent-with an induction of immune suppression (immunoparalysis), that can be measured by a systemic increase in the anti-inflammatory cytokine IL-10 (*30, 31*). Interestingly, there was significantly

increased *il-10* expression in WD- and KD-fed mice at 20 h p.i., compared to SC-fed mice (Fig 1F). Further, in septic patients, a high IL-10:TNF ratio equates with the clinical immunoparalytic phase and correlates with poorer sepsis outcomes (*32, 33*). Here we saw, WD- and KD-fed mice had significantly higher *il-10:tnf* ratios at 10 and 15 h compared to SC-fed mice (Fig 1G). These data conclude that mice exposed to diets enriched in SFAs show an initial hyper-inflammatory response to LPS, followed by an increased immunoparalytic phenotype, which correlates with enhanced disease severity, similar to what is seen in the clinic.

Diets enriched in SFAs drive enhanced responses to systemic LPS independent of the microbiome

We have previously shown that WD-fed mice experience increased endotoxemia severity and mortality independent of the microbiome (*1*). In order to confirm the increases in endotoxemia severity and mortality that correlated with KD were also independent of KD-associated microbiome changes, we used a germ free (GF) mouse model. Male and female C57BL/6 GF mice were fed SC, WD, and KD for 2 wk followed by injection with 50 mg/kg of LPS, our previously established LD_{50} for C57BL/6 GF mice injected with LPS (*1*). As we saw in the conventional mice, at 10 h p.i. WD- and KD-fed GF mice showed significant loss of body temperature, compared to SC-fed GF mice, indicating enhanced disease severity (Fig 2A). Additionally, WD- and KD-fed GF mice also displayed 100% mortality compared to only 50% mortality of SC-fed GF mice (Fig 2B). These data indicate that, similar to WD-fed mice, KD-associated increase in endotoxemia severity and mortality is independent of the microbiome.

Additionally, we next wanted to confirm that the hyper-inflammatory response to systemic LPS was independent of the WD- and KD-dependent microbiome, we measured systemic inflammation during endotoxemia via the expression of *tnf*, *il-6*, and *il-1β* in the blood at 0-10 h p.i. Similar to what we saw in conventional mice, WD- and KD-fed GF mice displayed significantly enhanced expression of *tnf, il-6*, and *il-1β* at 5h, compared to SC-fed GF mice (Fig 2C-E). Interestingly, *il-10* expression and *il-10:tnf* were not significantly different throughout all diets, suggesting the SFA-dependent enhanced immunoparalytic phenotype is dependent on the diet-associated microbiomes in WD- and KD-fed mice (Fig 2F, G). Together, these data suggest that the early hyper-inflammatory response, but not the late immunoparalytic response, to LPS associated with enriched dietary SFAs is independent of the diet-dependent microbiota.

Monocytes and splenocytes from KD-fed mice show a hyper-inflammatory response to LPS

It has been shown that circulating monocytes and splenocytes are necessary for induction of systemic inflammatory cytokines during endotoxemia (*26, 27*). Additionally, we see feeding a diet enriched only in SFAs (KD) leads to enhanced expression of *tnf* and *il-6* in the blood during endotoxemia (Fig 1C, D). However, it remains unclear if the KD induces *in vivo* reprogramming of monocytes and splenocytes leading to an enhanced response to LPS. Thus, we next sought out to determine if the chronic exposure to KD alters the response of monocytes and splenocytes to LPS *ex vivo*. First, we fed mice SC or KD for 2 wk (chronic exposure), isolated bone marrow monocytes (BMMs) from the femurs and tibias of mice and determined homeostatic inflammation of monocytes via expression of *tnf* and *il-6*. We found that prior to *ex vivo* LPS stimulation, BMMs isolated from mice chronically exposed to SC- or KD showed no significant difference in *tnf* expression, and *il-6* expression was significantly decreased in BMMs from KD-fed mice (Fig 3A). However, when BMMs were stimulated with LPS for 2h *ex vivo*, those from KD-fed mice showed significantly higher expression of *tnf* and *il-6* (Fig 3A). These data suggest that chronic exposure to KD does not enhance basal inflammatory status, but reprograms BMMs to respond with enhanced inflammation to LPS.

Similarly, we isolated splenocytes from SC- and KD-fed mice and found no difference between homeostatic inflammation of splenocytes between diets (0h), but an enhanced production of *tnf* in the splenocytes of KD-fed mice challenged with LPS, compared to splenocytes from SC-fed mice (Fig 3B). Together, these data suggest that BMMs and splenocytes from KD-fed mice are not inherently more inflammatory, but confer a hyper-inflammatory response to LPS, suggesting diets enriched in SFAs are inducing functional reprogramming of immune cells *in vivo*.

Palmitic acid (PA) and PA-associated fatty acids are enriched in the blood of KD-fed mice

Our data show that diets enriched in SFAs correlate with a hyper-inflammatory response to LPS *in vivo* and in *ex vivo* monocytes and splenocytes. We next wanted to identify target dietary SFAs enriched in the blood of mice that may be altering the host inflammatory response to LPS. It is known that the SFAs consumed in the diet determine the SFA profiles in the blood (*35-37*). Considering this, we used mass spectrometry lipidomics to create diet-dependent profiles of circulating fatty acids in SC- and KD-fed mice (*38*). Mice were fed SC or KD for 2 wk, then serum samples were collected via cardiac puncture and analyzed using qualitative

tandem liquid chromatography quadrupole time of flight mass spectrometry (LC-QToF MS/MS). We used principal component analysis (PCA) to visualize how samples within each data set clustered together according to diet, and how those clusters varied relative to one another in abundance levels of free fatty acids (FFA), triacylglycerols (TAG), and phosphatidylcholines (PC). For all three groups of FAs, individual mice grouped with members of the same diet represented by a 95% confidence ellipse with no overlap between SC- and KD-fed groups (Fig 4A-C). These data indicate that 2 wk of KD feeding is sufficient to significantly alter circulating FFAs, TAGs, and PCs, and that SC- and KD-fed mice display unique lipid blood profiles. Similarly, the relative abundance of sphingolipids (SG) in SC- and KD-fed mice displayed unique diet-dependent profiles with no overlapping clusters (Fig S2A). Though the independent role of each FFA, TAG, PC, and SG species has not been clinically defined, each are classes of lipids that when accumulated is associated with metabolic diseases, which have been shown to enhance susceptibility to sepsis and exacerbate inflammatory disease (*39-42*).

Importantly, we identified a significant increase in multiple circulating FFAs within the KD-fed mice, compared to the SC-fed mice, including a significant increase in free palmitic acid (PA; C16:0), a SFA that is found naturally in animal fats, vegetable oils, and human breast milk (*43*), and is enriched in both WD and KD (Table S1). Additionally, PA-containing TAGs and PCs were significantly elevated in KD-fed mice serum, compared to SC-fed mice (Fig 4D-G). These data indicate that KD feeding not only enhances levels of freely circulating PA, but also enhances the frequency PA is incorporated into other lipid species in the blood. Further, these data show that the KD induces significantly altered serum lipid profiles in mice within two weeks, and KD-dependent circulating fatty acids may have the potential to reprogram innate immune pathways that lead to a hyper-inflammatory response to LPS challenge.

Palmitic acid enhances macrophage response to LPS challenge

We have found free PA and PA-saturated lipids are significantly up-regulated in the blood of KD-fed mice, and both WD and KD are enriched in PA with 12% and 23% of total kcal respectively, whereas the SC contains only 3% PA (Table S1). Additionally, many groups have shown that PA induces expression and release of inflammatory cytokines in macrophages and monocytes (*28, 44*). Thus, we hypothesized PA may be the SFA mediating KD-dependent hyper-inflammatory response to LPS. We next wanted to determine if pre-

exposure to physiologically relevant concentrations of PA altered macrophage response during a secondary challenge with LPS. Serum PA levels can differ between people, and depend not only on fasting and postprandial states, but also metabolic health of the individual (*45, 46*). Current literature indicates a wide range of serum PA levels, between 0.7 and 3.6 mM, reflect a high-fat diet in humans (*47-50*). We aimed to use a physiologically relevant concentration of PA for our *in vitro* studies, and decided on 1mM in order to stay within a physiological range and avoid high levels of cytotoxicity in our macrophage model. Thus, we treated primary bone marrow-derived macrophages (BMDMs) with and without 1mM of PA for 12h, removed the media, subsequently treated with LPS (10 ng/mL) for an additional 24 h, and measured expression and release of TNF, IL-6, and IL-1β. We found that BMDMs pre-treated with 1mM of PA for 12 h and then with LPS expressed significantly higher levels of *tnf* and *il-6*, compared to naïve BMDMs treated with LPS (Fig 5A, B). *il-1β* expression was significantly lower in cells pre-treated with 1mM PA, suggesting a bifurcation in the temporal transcriptional regulation of *tnf/il-6* and *il-1β* by PA (Fig 5C). However, secretion of TNF, IL-6 and IL-1β were all enhanced in BMDMs pre-treated with 1mM of PA for 12 h (Fig 5 D-F). We found a similar hyper-inflammatory response to LPS in BMDMs treated with 1mM of PA for 24 h followed by LPS challenge (Fig 5G-I). Importantly, PA-treatment can induce apoptosis, however we found only 25% and 50% of PA-induced cell death at 12 h and 24 h, respectively, compared to our positive control (Cholera toxin B subunit; CTB and LPS) which showed 60% and 100% cytotoxicity at 12 h and 24 h (Fig S3A, B).

Considering 1mM concentration of PA reflects the higher range of physiologically relevant serum levels, we wanted to challenge BMDMs with a concentration of PA reflected in the lower range of physiologically relevant serum levels. Thus, we treated BMDMs with and without 0.5mM of PA for 12 h or 24 h, removed the media, subsequently treated with LPS (10 ng/mL) for an additional 24 h, and measured expression and secretion of TNF, IL-6, and IL-1β. We found that 12 and 24 h pre-treatment with 0.5mM of PA induced significantly higher expression of *tnf* and *il-6,* and *il-1β* after 24 h challenge with LPS, compared to naive BMDMs treated with LPS (Fig S4A-F). Thus, lower physiological levels of PA enhance production and secretion of inflammatory cytokines during secondary LPS challenge, further defining a novel role for PA in regulating a hyper-inflammatory response to a subsequent challenge with a microbial ligand.

Pentadecanoic acid (PDA, C15:0) is a SFA containing 1 less carbon than PA and is likewise found in milkfat, which is the primary fat source in the KD used in our *in vivo* studies. To understand if this hyper-

inflammatory response is specific to PA, we performed identical assays using a physiologically relevant concentration of PDA (50μM) followed by a secondary challenge with LPS (*50*). In accordance with our PA-treated BMDMs, 12 and 24 h PDA treatments resulted in significantly increased expression of *tnf, il-6, and il-1β* upon secondary stimulation with LPS (Fig S4G-L). This indicates that like PA, PDA alters macrophage responses and leads to significantly enhanced expression of inflammatory cytokines when challenged with LPS, suggesting this SFA-dependent regulation of macrophage response to LPS is not specific to PA. Together, these data show dietary SFAs common to both WD and KD have the capacity to alter the induction of inflammatory cytokines within macrophages upon secondary stimulation.

Palmitic acid is sufficient to increase endotoxemia severity and mortality.

Considering the drastic effect of PA on macrophage response to secondary LPS challenge, we next wanted to understand if PA is sufficient to induce a hyper-inflammatory response to LPS *in vivo*. We answered this question by first mimicking post-prandial systemic PA levels (1mM) by a single i.p. injection of ethyl palmitate and then challenging with LPS (i.p.) (*51*). Thus, mice were fed SC for 2 wk and then injected with a vehicle solution or ethyl palmitate (*51*). We rested the mice 12 h and then induced endotoxemia. PA-treated mice experienced increased endotoxemia severity as indicated by their significant decline in temperature compared to Veh mice (Fig 6A). Similar to WD- and KD-fed mice, PA-treated mice also exhibited 100% mortality, compared to 20% mortality seen in Veh mice (Fig 6B). Importantly, mice injected with PA for shorter time periods (0, 3, and 6 h) and then challenged with LPS did not exhibit increased disease severity or poor survival outcome (Fig S5A, B), concluding that a 12 h pre-treatment with PA is required for an increase in disease severity. Next, we measured systemic inflammatory status during endotoxemia via the expression of *tnf*, *il-6*, *il-1β*, and *il-10* in the blood between 0 and 20 h p.i. We found, similar to WD- and KD-fed mice, the 12 h PA-pre-treated mice showed significantly enhanced expression of *tnf* and *il-6* 5 h post-LPS challenge, compared to Veh control (Fig 6C, D). Expression of *il-1β* was moderately up-regulated in 2 of 3 12 h PA-pre-treated mice, compared to Veh-treated mice (Fig 6E). Thus, a 12 h pre-treatment with PA is sufficient to drive enhanced disease severity in mice challenged with LPS and that this PA-specific effect is dependent on length of exposure.

Enriched dietary PA induces trained immunity and resistance to fungal infection

Our data show that PA enhances endotoxemia severity *in vivo*, and enhances inflammatory responses of macrophages to a secondary and heterologous stimulus (LPS) *in vitro*. This form of regulation resembles trained immunity, which is described as "non-antigen specific innate immune cell memory"; however, it remains unclear if PA is inducing innate immune cell memory by priming or trained immunity. Priming occurs when the first stimulus enhances transcription of inflammatory genes and does not return to basal levels before the secondary stimulation (*52*). In contrast, trained immunity occurs when the first stimulus changes transcription of inflammatory genes, the immune status returns to basal levels, and challenge with a heterologous stimulus enhances transcription of inflammatory cytokines at much higher levels than those observed during the primary challenge (*52*). Thus, we evaluated the basal level expression of *tnf, il-6,* and *il-1β* in mice treated with 1mM of PA or Veh i.p. for 12h, before stimulation with LPS. Interestingly, we did not see significant differences in *tnf, il-6,* or *il-1β* expression at 12 h p.i. with PA (Fig 6F), which suggests that circulating immune cells of these mice were not in a primed state at these time points prior to LPS injection. Thus, we conclude that PA induces trained immunity, and not priming, however the time point of initial inflammation induced by PA remains unknown and most likely will be different for each inflammatory cytokine. Importantly, as a control we looked at LPS-induced hypoglycemia in PA-treated mice, and 12 h pre-treatment with PA did not alter LPS-induced hypoglycemia (Fig 6G), indicating that low blood glucose was not a driver of endotoxemia severity in 12 h PA mice.

Canonical inducers of non-antigen specific innate immune cell memory (e.g., BCG or β-glucan) induce long-lived enhanced innate immune responses to secondary inflammatory stimuli (*9, 53*). Considering WD followed by a reversion to SC has been shown to reprogram monocyte precursors in atherosclerotic mice long-term (*2*), we hypothesized that exposure to PA feeding would reprogram the inflammatory response *in vivo* and that this program would persist even after mice were "rested". In order to determine if PA alone can induce long-lived trained immunity, we injected SC mice with a vehicle solution or 1mM of PA i.p. once a day for 9 days (to mimic 1 high-fat meal per day) and then rested the mice for 1 wk (Veh or PA→SC). When challenged with systemic LPS, PA→SC showed an increase in endotoxemia severity and mortality compared to Veh→SC mice (Fig 6H-I), indicating that PA alone can induce long-lived immune memory.

Lastly, the most commonly studied models for inducing trained immunity are immunization with BCG or with β-glucan. These models of trained immunity have been shown to protect mice from systemic *Candida albicans* infection via lymphocyte-independent epigenetic alterations that lead to decreased kidney fungal burden (*54*). Thus, we next wanted to test if PA treatment induces lymphocyte-independent clearance of *C. albicans* infection. For these experiments, we treated in female Rag knockout ($Rag^{-/-}$) mice with or without PA for 12 h and subsequently infected i.v. with $2x10^6$ *C. albicans*. In accordance with canonical trained immunity models, mice treated with PA for 12 h showed a significant decrease in kidney fungal burden compared to Veh mice, 24 h post-infection (Fig 6J). These data find that PA is sufficient to induce lymphocyte-independent trained immunity *in vivo* and enhances host resistance to systemic *C. albicans* infection.

DISCUSSION

The impact of diet on inflammatory homeostasis is critical to understand when treating infection and diseases characterized by inflammation. Nutrient intake directly impacts cell function, and inflammatory responses of innate immune cells are not exempt from this level of regulation. Specifically, dietary SFAs have been shown to modulate inflammation of human monocytes and macrophages, which are the first responders in defense against infection and important producers of inflammatory cytokines during disease (*6, 44, 55-57*). Considering that SFAs make up a large portion of the WD, the most prevalent diet worldwide (*58*), it is therefore important to discover how they impact innate immune cell function and contribute to inflammatory disease progression and outcome.

In this study we showed WD- and KD-fed mice experience increased endotoxemia disease severity that correlates with an acute hyper-inflammatory response to LPS treatment, and poor survival outcome compared to SC-fed mice (Fig 1). Changes in blood glucose levels were not significant between WD-, KD- and SC-fed mice during disease, and artificially inducing ketosis in mice did not recapitulate the same results as KD feeding, indicating the KD-associated disease phenotypes are independent of hypoglycemic shock and ketosis (Fig S1). Furthermore, we repeated our experiments in GF mice fed the same diets, and showed that increased disease severity, enhanced inflammation, and poor survival still occurred in GF WD- and KD-fed mice, indicating that SFA-dependent disease phenotypes are also independent of diet-associated microbiota (Fig 2).

Immunoparalysis during sepsis is associated with high mortality rates in humans, and is indicated by enhanced *tnf:il-10* ratios in the blood (*32, 33*). Following the initial hyperinflammatory response to LPS-induced endotoxemia, WD- and KD-fed mice show significantly higher *tnf:il-10* ratios in their blood compared to SC-fed mice, indicating enhanced immunoparalysis. Interestingly, we found WD- and KD-fed GF mice did not show significant alterations in blood *tnf:il-10* ratios compared to SC-fed GF mice, and we conclude that SFA-dependent enhanced immunoparalysis is dependent on the microbiome (Fig 1G, 2G). It is important to explore other dietary constituents of SFA-enriched diets that may be altering the microbiota to drive immunoparalysis *in vivo*.

Other studies have highlighted the role of enriched dietary SFAs in driving disease severity. WD-fed atherosclerotic mice show long-term alterations to monocyte precursors in the bone marrow, and enhanced innate immune responses to LPS treatment (*2*). Additionally, short-term (3 day) KD-fed mice also exhibit enhanced endotoxemia-induced death (*5*). Our study adds to these compelling discoveries, and is unique in that we have found a specific dietary SFA associated with WD and KD that may be underlying immune regulation prior to and during disease. We used a lipidomics approach to determine the fatty acid profiles of blood in KD-fed mice, and showed significantly altered serum lipids compared to SC-fed mice. Interestingly, we found that many of the augmented lipids (TAGs, PCs, and SGs) were saturated with palmitic acid (C16:0; PA) (Fig 4, S2). PA is one of the most abundant SFAs in human serum, and has been found to be elevated in the blood of those with metabolic syndrome, diabetes and obesity (*50, 59-62*). This finding, along with our *ex vivo* LPS treatments of monocytes and splenocytes from KD-fed mice showing enhanced inflammatory cytokine expression compared to SC-fed mice, led us to consider the possibility that the higher levels of PA in the blood of KD-fed mice were modulating innate immune cells and enhancing their inflammatory response to heterologous stimuli. Our *in vitro* experiments corroborated this possibility, showing that primary macrophages pre-treated with higher and lower physiologically relevant levels of PA for 12–24 h induced a hyper-inflammatory response to subsequent LPS challenge (Fig 5).

Interestingly, physiologically relevant levels of a similarly sized SFA, pentadecanoic acid (PDA), also enhanced inflammatory cytokines during LPS challenge *in vitro* (Fig S4). Plasma levels of PDA are considered a biomarker for dietary intake of milkfat (*63*), and similar to PA, PDA is common to both WD and KD. Our findings indicate that SFA-dependent regulation of macrophage response to LPS is not specific to PA, and that

WD and KD contain multiple SFAs that are capable of reprogramming macrophages, and enhancing the response of inflammatory cytokines upon secondary stimulation with a microbial ligand. Therefore, WD and KD may contain cocktails of SFAs that induce trained immunity, and increase susceptibility to inflammatory diseases. Determining plasma concentrations of these immune modulating SFAs may be clinically useful as biomarkers for inflammatory disease vulnerability, and nutritional therapeutic interventions may be beneficial in preventing or treating disease.

It is possible that 1mM PA may be regulating levels of the Krebs Cycle metabolite, succinate, which has been shown to stabilize the transcription factor, HIF-1, and regulate IL-1β expression in macrophages (*64*). If PA disrupts the Krebs Cycle, this could lead to the accumulation of metabolites such as succinate, itaconate, or alpha-ketoglutarate, which are known to impact epigenetic markers associated with inflammatory regulation of macrophages (*65*). While PA has been shown to modulate macrophage metabolism (*28*), the impact of these alterations on the epigenome is unknown. The interplay between macrophage metabolism and epigenetics will be important to consider in future trained immunity studies where PA serves as the primary stimulus.

We found here that PA is capable of inducing non-antigen specific innate immune memory trained immunity, which is known to enhance monocyte and macrophage responses to homologous and/or heterologous stimuli (*52*). This would explain why diets high in PA correlate with hyper-inflammatory responses to LPS *in vivo*, and why PA-treated BMDMs show enhanced expression of inflammatory cytokines upon LPS treatment. Importantly, our work is the first to show that PA treatment followed by a 1wk resting period, both induce long-term immune reprogramming that leads to significantly impaired survival in mice with endotoxemia (Fig 6). Our findings also align well with recent studies that suggest diets enriched in SFAs induce trained immunity in an atherosclerotic mouse model, and non-microbial stimuli induce trained immunity in human monocytes (*2, 12, 13*).

Our findings here also align with the growing body of evidence indicating that trained immunity is a double-edged sword, where the phenomenon can be beneficial for resistance to infection, but detrimental in the context of inflammatory diseases (*10*). We conclude that PA-induced trained immunity may exacerbate the acute phase of sepsis and contribute to tissue damage brought on by enhanced inflammation. However, we are aware that trained immunity is a key feature of BCG vaccination, which has been shown to enhance innate

immune responses to subsequent infections, and may be responsible for increased resistance to severe COVID-19 (*8, 66*). Strikingly, we show here that $RAG^{-/-}$ mice injected with PA 12 h prior to *C. albicans* infection show significantly enhanced clearance of kidney fungal burden compared to Veh-injected $RAG^{-/-}$ mice. This is the first study to show that PA is capable of inducing non-antigen specific innate immune memory and enhancing inflammation that can be beneficial or detrimental depending on the disease state, and completely independent from mature lymphocytes.

PA-induced hyperinflammation, and enhanced disease severity and mortality in our sepsis mouse model, along with enhanced clearance of *Candida* infection independent of adaptive immunity, illuminates the complex nature of SFA-induced immune modulation. The potential for SFAs such as PA to directly impact innate immune metabolism, and epigenetics associated with inflammatory pathways, is paramount not only for dietary interventions, but also treatment of inflammatory diseases exacerbated by metabolic dysfunction in humans. How the interplay between metabolism and epigenetics influences sepsis severity and outcome remains unknown, and our study paves the way for the pursuit of dietary and immunometabolic interventions for the treatment of sepsis patients in a HFD-fed population.

MATERIALS AND METHODS

Cell lines and reagents. RAW 264.7 macrophages (from ATCC), BMDMs and BMMs were maintained in DMEM (Gibco) containing L-glutamine, sodium pyruvate, and high glucose supplemented with 10% heat-inactivated fetal bovine serum (FBS; GE Healthcare, SH3039603). BMDMs were also supplemented with 10% macrophage colony-stimulating factor (M-CSF; M-CSF-conditioned media was collected from NIH 3T3 cells expressing M-CSF, generously provided by Denise Monack at Stanford University).

Generation of BMDMs, BMMs, and splenocytes. Bone marrow-derived macrophages (BMDMs) and bone marrow-derived monocytes (BMMs) were harvested from the femurs and tibias of age-matched (6-8 wk) CO_2-euthanized female BALB/c mice. BMDM media was supplemented with 10% macrophage colony-stimulating factor (M-CSF) for differentiation, cells were seeded at 5 x 10^6 in petri dishes and cultured for 6 days, collected with cold PBS, and frozen in 90% FBS and 10% DMSO in liquid nitrogen for later use. BMMs were isolated from BMDM fraction using EasySep™ Mouse Monocyte Isolation Kit (STEMCELL). Spleens were harvested

from age-matched (6-8 wk) CO_2-euthanized female BALB/c mice, tissue was disrupted using the end of a syringe plunger on a 70 µm cell strainer and rinsed with FACS buffer (PBS + 2mM EDTA). Cells were subjected to red blood cell lysis with RBC lysing buffer (Sigma) followed by neutralization in FACS buffer.

Treatments. After thawing and culturing for 5 days, BMDMs were pelleted and resuspended in DMEM containing 5% FBS, 2% bovine serum albumin (BSA; Proliant Biologicals) and 10% M-CSF. Cells were seeded at 2.5 x 10^5 cells/well in 24-well tissue-culture plates, treated with EtOH 1.69%, 100 ng/mL LPS (Ultrapure LPS, *E. coli* 0111:B4, Invivogen), 500 µM or 1 mM palmitic acid (Sigma-Aldrich PHR112), 50 µM pentadecanoic acid (Sigma-Aldrich), or 36 µM behenic acid (Sigma-Aldrich) and incubated at 37°C and 5% CO_2 for 12 or 24 h. Next, cells were treated with an additional 10 ng/mL LPS or fatty acid as described above, and incubated an additional 24 h. RAW 264.7 macrophages thawed and cultured for 3-5 days, pelleted and resuspended in DMEM containing 5% FBS and 2% BSA, and treatments were identical to BMDM treatments. BMMs and were seeded immediately after harvesting at 4x10^^{5} cells/well in 96-well V-bottom plates in DMEM containing 10% FBS, and treated with LPS for 2 or 24 h. Splenocytes were seeded immediately after harvesting at 1 x 10^5 cells/well in 96-well V-bottom plates in RPMI media with L-glutamine (Cytiva) containing 10% FBS, and treated with LPS for 2 or 24 h. For all treatments, media was removed and cells were lysed with TRIzol (ThermoFisher), flash-frozen in liquid nitrogen, and stored at -80°C until qRT-PCR analysis. For all plates, all treatments were performed in triplicate.

Lactate dehydrogenase (LDH) assays. BMDMs were cultured as stated above and plated in 96-well tissue-culture plates at a concentration of 5 x 10^4 cells/well and incubated overnight. Cells were treated with ethanol, 20 µg/mL LPS, a mix of 20 µg/mL LPS and 20 µg/mL cholera toxin B (CTB) subunit (List Biological Labs), 1 mM PA, or a mix of 20 µg/mL LPS and 1mM PA in a phenol-red-free Optimem media (ThermoFisher) and incubated an additional 12 or 24 h. Supernatants were collected at the specified time points with LDH release quantified with a CytoTox96 Non-Radioactive Cytotoxicity Assay (Promega). Cytotoxicity was measured per well as a percentage of max LDH release, with background LDH release subtracted. For all plates, all treatments were performed in triplicate.

Measurement of cell viability. Cell viability was determined by 0.4% Trypan Blue dye exclusion test executed by TC20 Automated Cell Counter (Bio-Rad).

RNA extraction and real-time qPCR. Mice treated with PBS or LPS were sacrificed at specified time points and 10-20 µL of blood was collected from the tail vein, transferred into 50 µL of RNALater (ThermoFisher Scientific) and frozen at -80°C. RNA extractions were performed using RNeasy Mini Kit (Qiagen), cDNA was synthesized from RNA samples using SuperScript III First-Strand synthesis system (Invitrogen). Gene specific primers were used to amplify transcripts using FastStart Universal SYBR Green Master (Bio-Rad). A complete list of all primers used, including the names and sequences, is supplied as Supplementary Table 2.

Enzyme-linked immunosorbent assay (ELISA). TNF and IL-6 concentrations in mice serum were measured using TNF alpha and IL-6 Mouse ELISA Kits (ThermoFisher Scientific), according to the manufacturer's instructions. Absorbances were measured at a wavelength of 450 nm using a microplate reader (BioTek Synergy HTX).

Endotoxin-induced model of sepsis. Age-matched (6-8 wk) female BALB/c mice were anesthetized with isoflurane and injected subcutaneously with ID transponders (Bio Medic Data Systems). 2 wk post diet change, and 1 wk post ID transponder injection, mice were stimulated with a single injection of 6-10 mg/kg LPS reconstituted in endotoxin-free LAL reagent water (Invivogen) and diluted in PBS for a total volume of 200 µL. Control mice received corresponding volumes of PBS. Progression of disease was monitored every 2 h after LPS injection for clinical signs of endotoxin shock based on weight, coat and eyes appearance, level of consciousness and locomotor activity. Temperature was recorded using a DAS-8007 thermo-transponder wand (Bio Medic Data Systems). For PA injections, a solution of 750 mM ethyl palmitate (Millipore Sigma), 1.6% lecithin (Sigma-Aldrich) and 3.3% glycerol was made in endotoxin-free LAL reagent water (Lonza). The lecithin-glycerol-water solution was used as a vehicle, and mice were injected with 200 µL of the vehicle as a control, or ethyl palmitate solution to increase serum PA levels to 1 mM (*51*).

Mouse diets, glucose, and ketones. Six-week-old female mice were fed soft, irradiated chow and allowed to acclimate to research facility undisturbed for one week. Chow was replaced by Western Diet (Envigo, TD.88137), Ketogenic Diet (Envigo, TD.180423), or Standard Chow (Envigo, TD.08485) and mice were fed *ad libitum* for two weeks before induction of sepsis. For Ketogenic Diet, food was changed daily. For Western Diet, food was changed every 72 hours. Ketones and blood glucose were measured weekly and immediately prior to LPS injections with blood collected from the tail vein using Blood Ketone & Glucose Testing Meter (Keto-Mojo), or with urine collected on ketone indicator strips (One Earth Health, Ketone Test Strips).

Statistics analysis. Mann Whitney, Mantel-Cox, and student's t-tests were carried out with GraphPad Prism 9.0 software.

Ethical approval of animal studies. All animal studies were performed in accordance with National Institutes of Health (NIH) guidelines, the Animal Welfare Act, and US federal law. All animal experiments were approved by the Oregon Health and Sciences University Department of Comparative Medicine and were overseen by the Institutional Care and Use Committee (IACUC) under Protocol ID IP00001903. Animals were housed in a centralized research animal facility certified by Oregon Health and Science University. Conventional 8-10 wk-aged female BALB/c mice (Jackson Laboratory 000651) were used for the sepsis model, and isolation of BMDMs, BMMs, and splenocytes. GF male and female C57BL/6 mice (Oregon State University; bred in house) between 14 and 23 wk old were used for the GF sepsis model. BALB/c Rag1$^{-/-}$ mice between 8 and 24 wk were infected i.v. with 2x10^{6} CFUs of *C. albicans* SC5314 (ATCC #MYA-2876) and kidney fungal burden was assessed 24 h post-infection. Kidneys were harvested 24 h post-infection and homogenized organs were plated in serial dilutions on Yeast Peptone Dextrose plates to assess fungal burden.

Lipidomics PCA Analysis

Mice on specialized diets were sacrificed at the indicated time points after PBS or LPS treatment with 300-600µL of blood collected via cardiac puncture into heparinized tubes. Blood samples were centrifuged for 15 minutes at 2,500rpm at 4°C and plasma was transferred to a new tube before storage at -80°C. Plasma samples were analyzed via LC-MS/MS. Lipidomic data sets were scaled using the *scale* function and principal

component analyses were performed using the *prcomp* function from the stats package in R Version 3.6.2. Visualization of PCAs and biplots was performed with the *fviz_pca_ind* and *fviz_pca_biplot* functions from the factoextra package and with the *ggplot2* package (*67, 68*). For each diet group, 95% confidence ellipses were plotted around the group mean using the *coord.ellipse* function from the FactoMineR package (*69*). Heatmaps were created using the *pheatmap* package (*70*).

ACKNOWLEDGEMENTS

We would like to thank Ajesh Saini, a student in the Napier Lab, for his contributions in carrying out the ELISA data within this manuscript. This study was supported by National Institute of General Medical Sciences (NIGMS) grant 5R35GM133804-02 to B.A.N.

FIGURE LEGENDS

Fig. 1 HFDs lead to enhanced endotoxemia severity and altered systemic inflammatory profiles. Age-matched (4-6 wk) mice were fed SC, WD, or KD for 2 wk and injected i.p. with 6 mg/kg of LPS. **a** Temperature loss and **b** survival were monitored every 2 h. At indicated times 10-20 µL of blood was drawn via the tail vein, RNA was collected, and samples were assessed for expression of **c** *tnf,* **d** *il-6,* **e** *il-1β,* and **f** *il-10* via qRT-PCR. **g** *il-10:tnf* ratio was calculated for 5, 10, 15, and 20 hours p.i. with LPS. For **a-g**, data are representative of 1 experiment, n=5 mice per diet group. For **a** and **c-g** a Mann Whitney test was used for pairwise comparisons. For **b** a log-rank Mantel-Cox test was used for survival curve comparison. For all panels, *$p< 0.05$; **$p < 0.01$; ***$p< 0.001$. For panels **c-e**, Φ symbols indicate WD significance and ∞ symbols indicate KD significance. Error bars show mean ± SD.

Fig. 2 KD-dependent increase in endotoxemia severity and mortality is independent of the KD-induced microbiome. 19-23 wk old female and 14-23 wk old male germ-free C57BL/6 mice were fed SC, WD, or KD for 2 wk and injected i.p. with 50 mg/kg of LPS. **a** Temperature loss and **b** survival were monitored every 5 h

p.i. **c-e** At indicated times, 10-20 µL of blood was drawn via the tail vein, RNA was collected, and samples were assessed for expression of **c** *tnf,* **d** *il-6,* **e** *il-1β,* and **f** *il-10* via qRT-PCR. SC, n=6; WD, n= 5, and KD, n= 9. For **a,** and **c-g** a Mann Whitney test was used for pairwise comparisons. For **b** a log-rank Mantel-Cox test was used for survival curve comparison. For all panels, **p*< 0.05; ***p* < 0.01; ****p*< 0.001. For **c-e**, Φ symbols indicate WD significance and ∞ symbols indicate KD significance. Error bars shown mean ± SD.

Fig. 3 Monocytes and splenocytes from KD-fed mice show a hyper-inflammatory response to LPS *ex vivo*. Age-matched (4-6 wk) mice fed SC or KD for 2 weeks. Monocytes were isolated from the femurs and tibias of mice and plated at 4x10^^{6} cells/mL. RNA was extracted from **a** untreated monocytes (0 h) or monocytes treated with or without LPS (10 ng/mL) for 2 h. Expression of *tnf* and *il-16* was analyzed via qRT-PCR. Splenocytes were isolated and plated at 1x10^^{6} cells/mL. RNA was isolated from **b** untreated splenocytes (0 h) or splenocytes treated with or without LPS (10 ng/mL) for 2h. Expression of *tnf* and *il-6* was analyzed via qRT-PCR. *n* = 5 mice/group in each representative experiment. A student's t-test was used for statistical significance. For all panels, * $p < 0.05$; ** $p < 0.01$; *** $p < 0.001$; **** $p < 0.0001$.

Fig. 4 Principal component analysis (PCA) and heatmap analysis of lipidomic data in SC- and KD-fed mouse plasma samples. Data points represent single animal samples and colors represent groups fed SC (black) or KD (orange) diets for two weeks and a 95% confidence ellipse was constructed around the mean point of each group for **a** free fatty acids, **b** triglycerides (B), and **c** phosphatidylcholines. Heatmaps analysis of **d** free fatty acids, **e** triglycerides, and **f** phosphatidylcholines in SC and KD mice. Lipid components containing 16:0 palmitic chains are highlighted in purple and components that are significantly different between the two groups are in bold. **g** Comparison of palmitic acid 16:0 peak area detected by LC-MS/MS between SC and KD groups. For **d-g,** statistical significance determined by unpaired two-tailed t-test between SC and KD groups. For all panels, *, $p < 0.05$; **, $p < 0.01$; ***, $p < 0.001$. n=3 per group.

Fig. 5 Physiological levels of PA induce a hyper-inflammatory response to secondary challenge with LPS in macrophages. Primary bone marrow-derived macrophages (BMDMs) were isolated from aged-matched female and male mice. BMDMs were plated at treated with either ethanol (EtOH; media with 1.69%

ethanol), media (Ctrl for LPS), or LPS (100 ng/mL) for 12 h, or palmitic acid (PA; 1mM; diluted in 1.69% EtOH) for 12 h, with and without a secondary challenge with LPS. After indicated time points, RNA was isolated and expression of **a** *tnf*, **b** *il-6*, **c** il-*1β* was measured via qRT-PC or supernatants were assessed via ELISA for **d** TNF, **e** IL-6, and **f** IL-1β secretion. Additionally, BMDMs were treated with either EtOH, media, or LPS (10 ng/mL) for 24 h, or PA (1mM; diluted in 1.69% EtOH) for 24 h, with and without a secondary challenge with LPS. After indicated time points, RNA was isolated and expression of **g** *tnf*, **h** *il-6*, **i** il-*1β* was measured via qRT-PCR. For all plates, all treatments were performed in triplicate. For all panels, a student's *t*-test was used for statistical significance. **, p < 0.05; **, p < 0.01; ***, p < 0.001; ****, p < 0.0001.* For all panels, error bars show the mean ± SD.

Fig. 6 PA is a novel mediator of trained immunity and is sufficient for inducing a hyper-inflammatory response to LPS and enhanced clearance of *Candida albicans* infection. Age-matched (4-6 wk) female mice were fed SC for 2 wk and injected i.p. with ethyl palmitate (PA, 750mM) or vehicle (Veh) solutions 12 h before i.p. LPS injections (10 mg/kg). **a** Temperature loss was monitored every 2 h as a measure of disease severity or **b** survival. At indicated times 10-20 µL of blood was drawn via the tail vein, RNA was collected, and samples were assessed for expression of **c** *tnf,* **d** *il-6,* and **e** *il-1β* via qRT-PCR. **f** Blood was collected via the tail vein from Vehicle (Veh) and PA pre-treated (12 h PA) mice immediately prior to LPS injection and samples were assessed for expression of *tnf, il-6, il-1β*, and *il-10* via qRT-PCR. **g** Blood was collected via the tail vein from Veh (V) and 12 h PA (PA) 0 and 20 h p.i. with LPS to measure blood glucose levels. Additionally, mice were injected i.v. with ethyl palmitate (PA, 750mM) or vehicle (Veh) solutions every day for 9 days and then rested for 7 days before LPS injections (10 mg/kg). **h** Temperature loss and **j** survival were monitored during endotoxemia. **j** Age-matched (8-9 wk) female $RAG^{-/-}$ mice were injected i.v. with ethyl palmitate (PA, 750mM) or vehicle (Veh) solutions 12 h before *C. albicans* infection. Fungal burden of kidneys from Vehicle (Veh) and PA pre-treated (12 h PA) mice 24 h after *C. albicans* infection. For **a-i** data are representative of 2 experiments and *n* = 5 mice/group. For **j** data are representative of 2 experiments and *n* = 6 mice/group For **a**, **c-h,** and **j,** a Mann Whitney test was used for pairwise comparisons. For **b** and **i,** a log-rank Mantel-Cox test was used for survival curve comparison. For all panels, *, $p < 0.05$; **, $p < 0.01$; ***, $p < 0.001$; ****, $p < 0.0001$.

REFERENCES

1. B. A. Napier *et al.*, Western diet regulates immune status and the response to LPS-driven sepsis independent of diet-associated microbiome. *Proc Natl Acad Sci U S A* **116**, 3688-3694 (2019).
2. A. Christ *et al.*, Western Diet Triggers NLRP3-Dependent Innate Immune Reprogramming. *Cell* **172**, 162-175.e114 (2018).
3. E. N. Komegae *et al.*, Site-Specific Reprogramming of Macrophage Responsiveness to Bacterial Lipopolysaccharide in Obesity. *Front Immunol* **10**, 1496 (2019).
4. J. D. Short *et al.*, Dyslipidemic Diet-Induced Monocyte "Priming" and Dysfunction in Non-Human Primates Is Triggered by Elevated Plasma Cholesterol and Accompanied by Altered Histone Acetylation. *Front Immunol* **8**, 958 (2017).
5. A. Wang *et al.*, Opposing Effects of Fasting Metabolism on Tissue Tolerance in Bacterial and Viral Inflammation. *Cell* **166**, 1512-1525.e1512 (2016).
6. L. Haversen, K. N. Danielsson, L. Fogelstrand, O. Wiklund, Induction of proinflammatory cytokines by long-chain saturated fatty acids in human macrophages. *Atherosclerosis* **202**, 382-393 (2009).

7. E. A. Schwartz *et al.*, Nutrient modification of the innate immune response: a novel mechanism by which saturated fatty acids greatly amplify monocyte inflammation. *Arterioscler Thromb Vasc Biol* **30**, 802-808 (2010).

8. M. G. Netea *et al.*, Trained immunity: A program of innate immune memory in health and disease. *Science* **352**, aaf1098 (2016).

9. M. G. Netea *et al.*, Defining trained immunity and its role in health and disease. *Nat Rev Immunol* **20**, 375-388 (2020).

10. A. R. DiNardo, M. G. Netea, D. M. Musher, Postinfectious Epigenetic Immune Modifications - A Double-Edged Sword. *N Engl J Med* **384**, 261-270 (2021).

11. A. Christ, E. Latz, The Western lifestyle has lasting effects on metaflammation. *Nat Rev Immunol* **19**, 267-268 (2019).

12. S. Bekkering *et al.*, Oxidized low-density lipoprotein induces long-term proinflammatory cytokine production and foam cell formation via epigenetic reprogramming of monocytes. *Arterioscler Thromb Vasc Biol* **34**, 1731-1738 (2014).

13. M. van Splunter *et al.*, Induction of Trained Innate Immunity in Human Monocytes by Bovine Milk and Milk-Derived Immunoglobulin G. *Nutrients* **10**, (2018).

14. G. S. Hotamisligil, Foundations of Immunometabolism and Implications for Metabolic Health and Disease. *Immunity* **47**, 406-420 (2017).

15. H. Wen *et al.*, Fatty acid-induced NLRP3-ASC inflammasome activation interferes with insulin signaling. *Nat Immunol* **12**, 408-415 (2011).

16. M. T. Nguyen *et al.*, A subpopulation of macrophages infiltrates hypertrophic adipose tissue and is activated by free fatty acids via Toll-like receptors 2 and 4 and JNK-dependent pathways. *J Biol Chem* **282**, 35279-35292 (2007).

17. H. Charles-Messance, K. A. J. Mitchelson, E. De Marco Castro, F. J. Sheedy, H. M. Roche, Regulating metabolic inflammation by nutritional modulation. *J Allergy Clin Immunol* **146**, 706-720 (2020).

18. E. L. Goldberg *et al.*, Ketogenic diet activates protective γδ T cell responses against influenza virus infection. *Sci Immunol* **4**, (2019).

19. M. P. Fink, Animal models of sepsis. *Virulence* **5**, 143-153 (2014).

20. B. A. Napier *et al.*, Complement pathway amplifies caspase-11-dependent cell death and endotoxin-induced sepsis severity. *J Exp Med*, (2016).

21. H. Saito, E. R. Sherwood, T. K. Varma, B. M. Evers, Effects of aging on mortality, hypothermia, and cytokine induction in mice with endotoxemia or sepsis. *Mech Ageing Dev* **124**, 1047-1058 (2003).

22. C. F. Raetzsch *et al.*, Lipopolysaccharide inhibition of glucose production through the Toll-like receptor-4, myeloid differentiation factor 88, and nuclear factor kappa b pathway. *Hepatology* **50**, 592-600 (2009).

23. J. P. Filkins, R. P. Cornell, Depression of hepatic gluconeogenesis and the hypoglycemia of endotoxin shock. *Am J Physiol* **227**, 778-781 (1974).

24. L. Laffel, Ketone bodies: a review of physiology, pathophysiology and application of monitoring to diabetes. *Diabetes Metab Res Rev* **15**, 412-426 (1999).

25. A. J. Lewis, C. W. Seymour, M. R. Rosengart, Current Murine Models of Sepsis. *Surg Infect (Larchmt)* **17**, 385-393 (2016).

26. Y. V. Radzyukevich, N. I. Kosyakova, I. R. Prokhorenko, Participation of Monocyte Subpopulations in Progression of Experimental Endotoxemia (EE) and Systemic Inflammation. *Journal of Immunology Research* **2021**, 1-9 (2021).

27. L. Zhang *et al.*, Splenocyte Apoptosis and Autophagy Is Mediated by Interferon Regulatory Factor 1 During Murine Endotoxemia. *Shock* **37**, 511-517 (2012).

28. G. I. Lancaster *et al.*, Evidence that TLR4 Is Not a Receptor for Saturated Fatty Acids but Mediates Lipid-Induced Inflammation by Reprogramming Macrophage Metabolism. *Cell Metab* **27**, 1096-1110.e1095 (2018).

29. J. D. Schilling *et al.*, Palmitate and Lipopolysaccharide Trigger Synergistic Ceramide Production in Primary Macrophages. *Journal of Biological Chemistry* **288**, 2923-2932 (2013).

30. S. C. Cheng *et al.*, Broad defects in the energy metabolism of leukocytes underlie immunoparalysis in sepsis. *Nat Immunol* **17**, 406-413 (2016).

31. C. Nedeva, J. Menassa, H. Puthalakath, Sepsis: Inflammation Is a Necessary Evil. *Front Cell Dev Biol* **7**, 108 (2019).

32. C. A. Gogos, E. Drosou, H. P. Bassaris, A. Skoutelis, Pro- versus anti-inflammatory cytokine profile in patients with severe sepsis: a marker for prognosis and future therapeutic options. *J Infect Dis* **181**, 176-180 (2000).

33. J. T. van Dissel, P. van Langevelde, R. G. Westendorp, K. Kwappenberg, M. Frölich, Anti-inflammatory cytokine profile and mortality in febrile patients. *Lancet* **351**, 950-953 (1998).

34. S. Saeed *et al.*, Epigenetic programming of monocyte-to-macrophage differentiation and trained innate immunity. *Science* **345**, 1251086 (2014).

35. R. M. Dougherty, C. Galli, A. Ferro-Luzzi, J. M. Iacono, Lipid and phospholipid fatty acid composition of plasma, red blood cells, and platelets and how they are affected by dietary lipids: a study of normal subjects from Italy, Finland, and the USA. *Am J Clin Nutr* **45**, 443-455 (1987).

36. C. M. Skeaff, L. Hodson, J. E. McKenzie, Dietary-induced changes in fatty acid composition of human plasma, platelet, and erythrocyte lipids follow a similar time course. *J Nutr* **136**, 565-569 (2006).

37. N. Zollner, F. Tato, Fatty acid composition of the diet: impact on serum lipids and atherosclerosis. *Clin Investig* **70**, 968-1009 (1992).

38. J. Choi *et al.*, Comprehensive analysis of phospholipids in the brain, heart, kidney, and liver: brain phospholipids are least enriched with polyunsaturated fatty acids. *Mol Cell Biochem* **442**, 187-201 (2018).

39. P. J. Meikle, S. A. Summers, Sphingolipids and phospholipids in insulin resistance and related metabolic disorders. *Nat Rev Endocrinol* **13**, 79-91 (2017).

40. I. S. S. A, A. B. C, J. S. A, Changes in Plasma Free Fatty Acids Associated with Type-2 Diabetes. *Nutrients* **11**, (2019).

41. E. Sokolowska, A. Blachnio-Zabielska, The Role of Ceramides in Insulin Resistance. *Front Endocrinol (Lausanne)* **10**, 577 (2019).

42. M. Papadimitriou-Olivgeris *et al.*, The Role of Obesity in Sepsis Outcome among Critically Ill Patients: A Retrospective Cohort Analysis. *Biomed Res Int* **2016**, 5941279 (2016).

43. A. Mancini *et al.*, Biological and Nutritional Properties of Palm Oil and Palmitic Acid: Effects on Health. *Molecules* **20**, 17339-17361 (2015).

44. J. Korbecki, K. Bajdak-Rusinek, The effect of palmitic acid on inflammatory response in macrophages: an overview of molecular mechanisms. *Inflamm Res* **68**, 915-932 (2019).

45. V. Salomaa *et al.*, Fatty acid composition of serum cholesterol esters in different degrees of glucose intolerance: A population-based study. *Metabolism* **39**, 1285-1291 (1990).

46. B. Vessby *et al.*, The Risk to Develop NIDDM Is Related to the Fatty Acid Composition of the Serum Cholesterol Esters. *Diabetes* **43**, 1353-1357 (1994).

47. L. Liu *et al.*, Targeted metabolomic analysis reveals the association between the postprandial change in palmitic acid, branched-chain amino acids and insulin resistance in young obese subjects. *Diabetes Res Clin Pract* **108**, 84-93 (2015).

48. S. F. Gallego, M. Hermansson, G. Liebisch, L. Hodson, C. S. Ejsing, Total Fatty Acid Analysis of Human Blood Samples in One Minute by High-Resolution Mass Spectrometry. *Biomolecules* **9**, (2018).

49. C. D. C. Buchanan *et al.*, Analysis of major fatty acids from matched plasma and serum samples reveals highly comparable absolute and relative levels. *Prostaglandins, Leukotrienes and Essential Fatty Acids* **168**, 102268 (2021).

50. M. Perreault *et al.*, A distinct fatty acid profile underlies the reduced inflammatory state of metabolically healthy obese individuals. *PLoS One* **9**, e88539 (2014).

51. K. Eguchi *et al.*, Saturated fatty acid and TLR signaling link beta cell dysfunction and islet inflammation. *Cell Metab* **15**, 518-533 (2012).

52. M. Divangahi *et al.*, Trained immunity, tolerance, priming and differentiation: distinct immunological processes. *Nat Immunol* **22**, 2-6 (2021).

53. E. Kaufmann *et al.*, BCG Educates Hematopoietic Stem Cells to Generate Protective Innate Immunity against Tuberculosis. *Cell* **172**, 176-190 e119 (2018).

54. J. Kleinnijenhuis *et al.*, Bacille Calmette-Guerin induces NOD2-dependent nonspecific protection from reinfection via epigenetic reprogramming of monocytes. *Proc Natl Acad Sci U S A* **109**, 17537-17542 (2012).

55. M. A. Gianfrancesco *et al.*, Saturated fatty acids induce NLRP3 activation in human macrophages through K(+) efflux resulting from phospholipid saturation and Na, K-ATPase disruption. *Biochim Biophys Acta Mol Cell Biol Lipids* **1864**, 1017-1030 (2019).

56. L. L'Homme *et al.*, Unsaturated fatty acids prevent activation of NLRP3 inflammasome in human monocytes/macrophages. *J Lipid Res* **54**, 2998-3008 (2013).

57. M. Riera-Borrull, et al., Palmitate conditions macrophages for enhanced responses toward inflammatory stimuli via JNK activation. *Journal of Immunology*, (2017).

58. L. Cordain *et al.*, Origins and evolution of the Western diet: health implications for the 21st century. *Am J Clin Nutr* **81**, 341-354 (2005).

59. G. V. Richieri, A. M. Kleinfeld, Unbound free fatty acid levels in human serum. *J Lipid Res* **36**, 229-240 (1995).

60. Z. D. Alsharari *et al.*, Serum Fatty Acids, Desaturase Activities and Abdominal Obesity - A Population-Based Study of 60-Year Old Men and Women. *PLoS One* **12**, e0170684 (2017).

61. E. Warensjo, U. Riserus, B. Vessby, Fatty acid composition of serum lipids predicts the development of the metabolic syndrome in men. *Diabetologia* **48**, 1999-2005 (2005).

62. J. M. Bruun *et al.*, Higher production of IL-8 in visceral vs. subcutaneous adipose tissue. Implication of nonadipose cells in adipose tissue. *Am J Physiol Endocrinol Metab* **286**, E8-13 (2004).

63. B. Jenkins, J. A. West, A. Koulman, A review of odd-chain fatty acid metabolism and the role of pentadecanoic Acid (c15:0) and heptadecanoic Acid (c17:0) in health and disease. *Molecules* **20**, 2425-2444 (2015).

64. G. M. Tannahill *et al.*, Succinate is an inflammatory signal that induces IL-1beta through HIF-1alpha. *Nature* **496**, 238-242 (2013).

65. D. G. Ryan, L. A. J. O'Neill, Krebs Cycle Reborn in Macrophage Immunometabolism. *Annu Rev Immunol* **38**, 289-313 (2020).

66. L. E. Escobar, A. Molina-Cruz, C. Barillas-Mury, BCG vaccine protection from severe coronavirus disease 2019 (COVID-19). *Proc Natl Acad Sci U S A* **117**, 17720-17726 (2020).

67. A. K. F. Mundt *et al.* Factoextra: Extract and visualize the results of multivariate data analysis. *R package v1.0.5*, 337.354 (2017).

68. H. Wickham. *ggplot2: Elegant graphics for data analysis.* Springer Publishing Group (2016).

69. S. Lê *et al.*, FactoMineR:an R package for multivariate analysis. *Journal of Statistical Software* (2008).

52 70. R. Kolde *et al.* Host genetic variation and its microbiome interactions within the Human Microbiome
53 Project. *Genome Med* 10: 6 (2018).

54

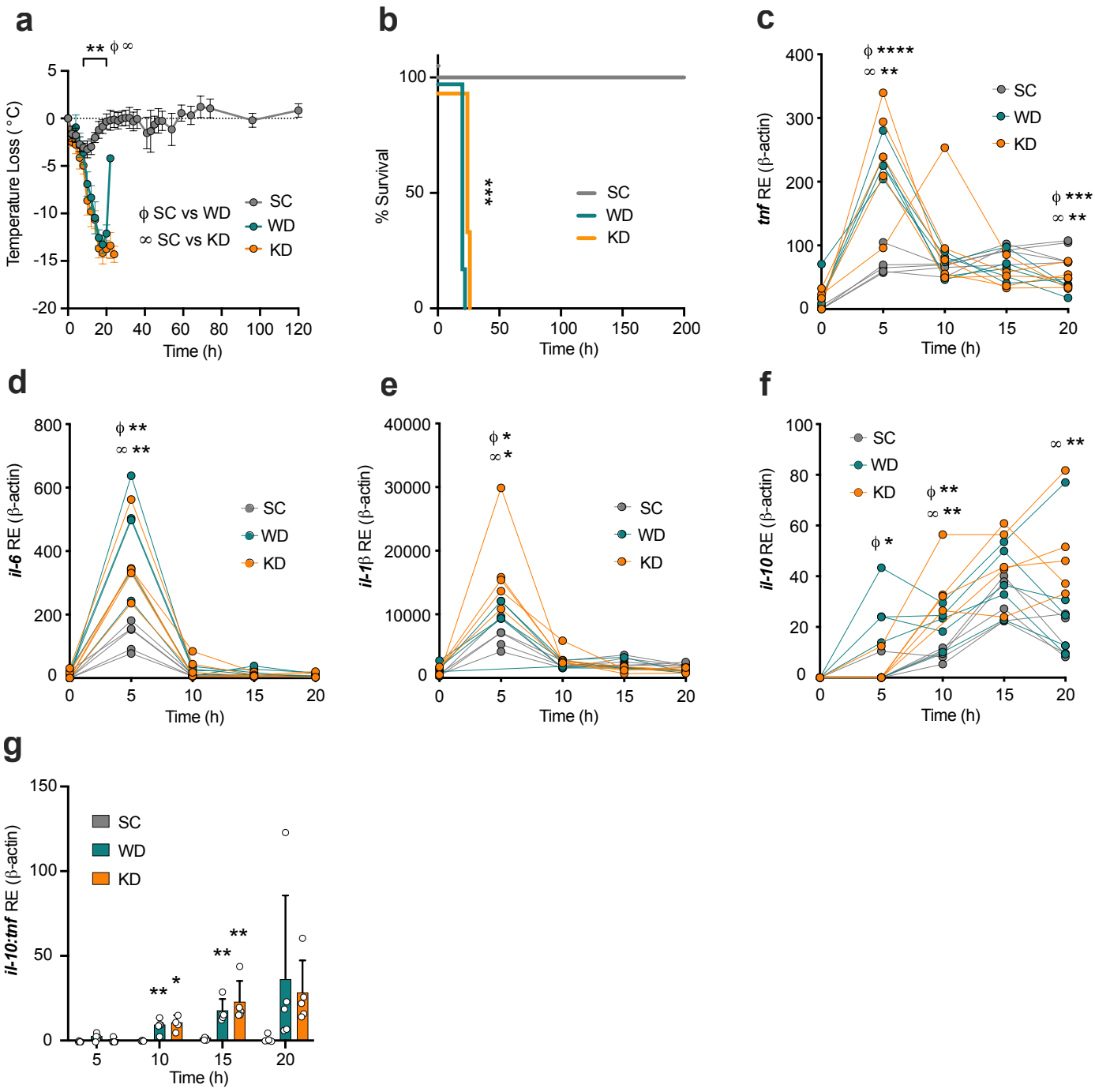
a
** ϕ ∞
Temperature Loss (°C)
ϕ SC vs WD
∞ SC vs KD
SC
WD
KD
Time (h)
b
% Survival
***
SC
WD
KD
Time (h)
c
ϕ ****
∞ **
ϕ ***
∞ **
tnf RE (β-actin)
SC
WD
KD
Time (h)
d
ϕ **
∞ **
il-6 RE (β-actin)
SC
WD
KD
Time (h)
e
ϕ *
∞ *
il-1β RE (β-actin)
SC
WD
KD
Time (h)
f
ϕ *
ϕ **
∞ **
∞ **
il-10 RE (β-actin)
SC
WD
KD
Time (h)
g
il-10:tnf RE (β-actin)
SC
WD
KD
Time (h)

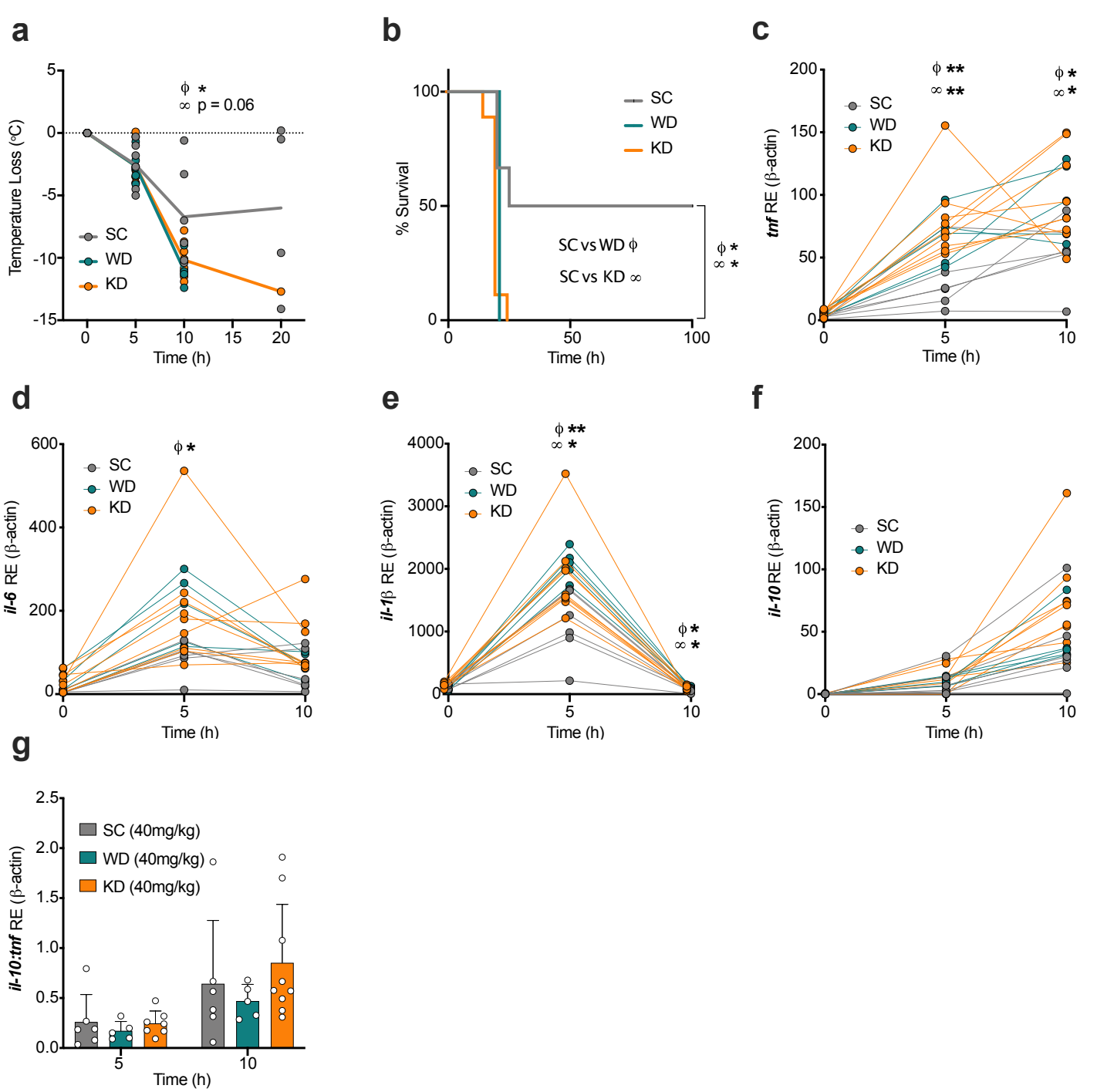
a
Temperature Loss (°C)
Time (h)
ϕ *
∞ p = 0.06
SC
WD
KD
b
% Survival
Time (h)
SC vs WD ϕ
SC vs KD ∞
ϕ *
∞ *
c
tnf RE (β-actin)
Time (h)
ϕ **
∞ **
ϕ *
∞ *
d
il-6 RE (β-actin)
Time (h)
ϕ *
e
il-1β RE (β-actin)
Time (h)
ϕ **
∞ *
ϕ *
∞ *
f
il-10 RE (β-actin)
Time (h)
g
il-10:tnf RE (β-actin)
Time (h)
SC (40mg/kg)
WD (40mg/kg)
KD (40mg/kg)

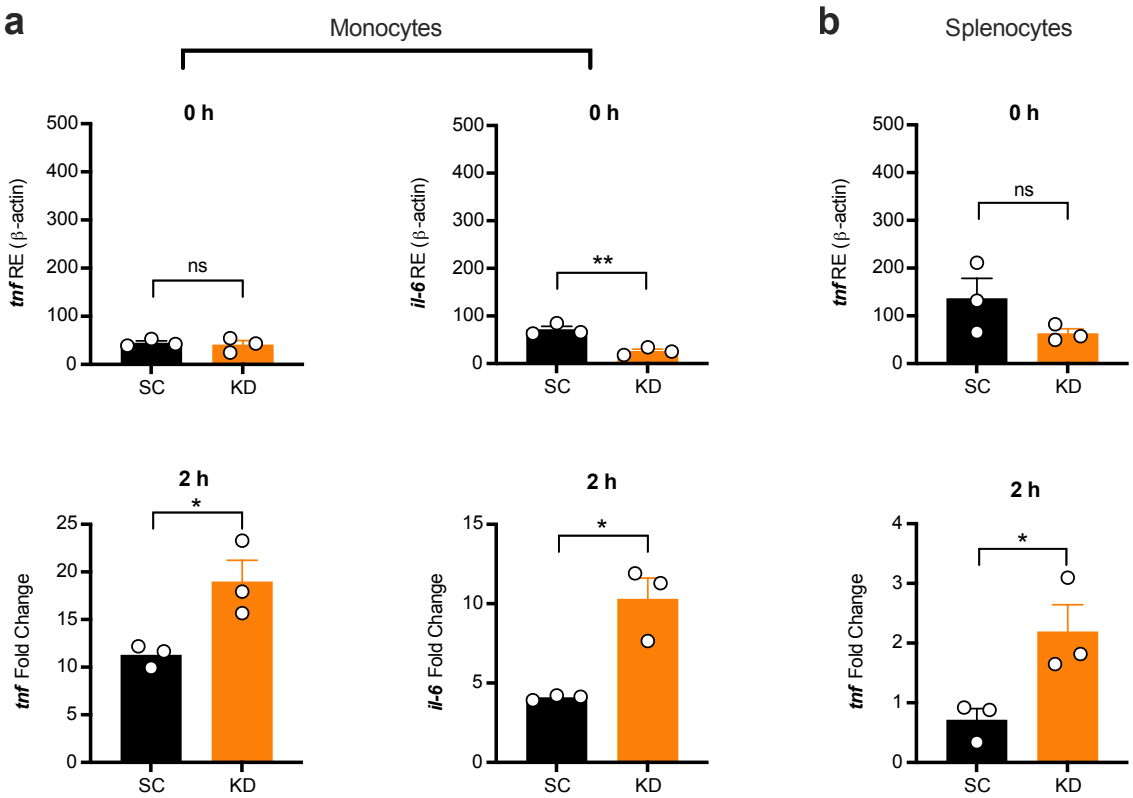
a
Monocytes
b
Splenocytes
0 h
2 h
tnf RE (β-actin)
il-6 RE (β-actin)
tnf Fold Change
il-6 Fold Change
ns
**
*
SC
KD
0
100
200
300
400
500
5
10
15
20
25
1
2
3
4

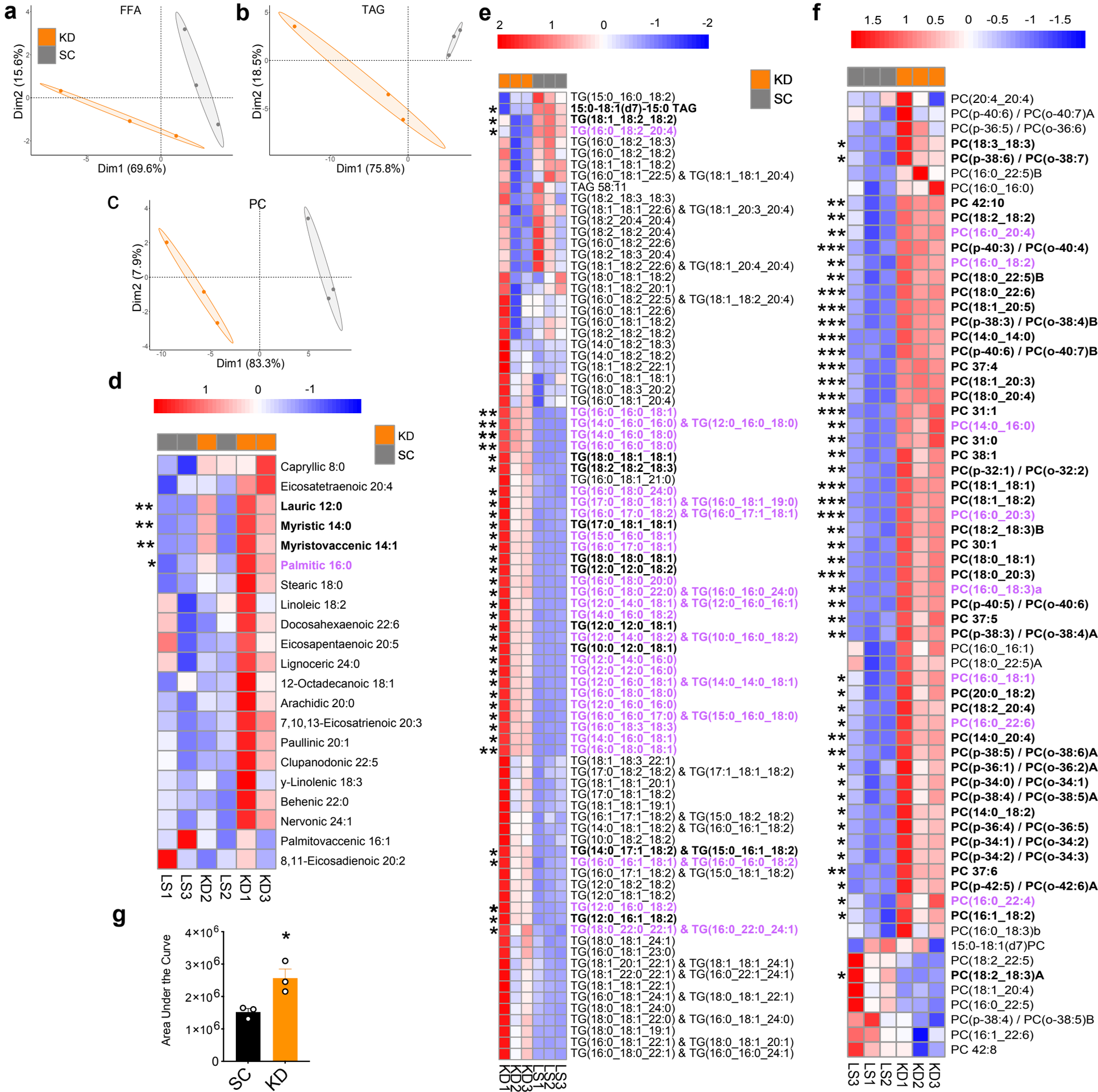
a
FFA
KD
SC
Dim2 (15.6%)
Dim1 (69.6%)
b
TAG
Dim2 (18.5%)
Dim1 (75.8%)
c
PC
Dim2 (7.9%)
Dim1 (83.3%)
d
1 0 -1
KD
SC
Capryllic 8:0
Eicosatetraenoic 20:4
Lauric 12:0
Myristic 14:0
Myristovaccenic 14:1
Palmitic 16:0
Stearic 18:0
Linoleic 18:2
Docosahexaenoic 22:6
Eicosapentaenoic 20:5
Lignoceric 24:0
12-Octadecanoic 18:1
Arachidic 20:0
7,10,13-Eicosatrienoic 20:3
Paullinic 20:1
Clupanodonic 22:5
y-Linolenic 18:3
Behenic 22:0
Nervonic 24:1
Palmitovaccenic 16:1
8,11-Eicosadienoic 20:2
LS1 LS3 KD2 LS2 KD1 KD3
e
2 1 0 -1 -2
KD
SC
TG(15:0_16:0_18:2)
15:0-18:1(d7)-15:0 TAG
TG(18:1_18:2_18:2)
TG(16:0_18:2_20:4)
TG(16:0_18:2_18:3)
TG(16:0_18:2_18:2)
TG(18:1_18:1_18:2)
TG(16:0_18:1_22:5) & TG(18:1_18:1_20:4)
TAG 58:11
TG(18:2_18:3_18:3)
TG(18:1_18:1_22:6) & TG(18:1_20:3_20:4)
TG(18:2_20:4_20:4)
TG(18:2_18:2_20:4)
TG(16:0_18:2_22:6)
TG(18:2_18:3_20:4)
TG(18:1_18:2_22:6) & TG(18:1_20:4_20:4)
TG(18:0_18:1_18:2)
TG(18:1_18:2_20:1)
TG(16:0_18:2_22:5) & TG(18:1_18:2_20:4)
TG(16:0_18:1_22:6)
TG(16:0_18:1_18:2)
TG(18:2_18:2_18:2)
TG(14:0_18:2_18:3)
TG(14:0_18:2_18:2)
TG(18:1_18:2_22:1)
TG(16:0_18:1_18:1)
TG(18:0_18:3_20:2)
TG(16:0_18:1_20:4)
TG(16:0_16:0_18:1)
TG(14:0_16:0_16:0) & TG(12:0_16:0_18:0)
TG(14:0_16:0_18:0)
TG(16:0_16:0_18:0)
TG(18:0_18:1_18:1)
TG(18:2_18:2_18:3)
TG(16:0_18:1_21:0)
TG(16:0_18:0_24:0)
TG(17:0_18:0_18:1) & TG(16:0_18:1_19:0)
TG(16:0_17:0_18:2) & TG(16:0_17:1_18:1)
TG(17:0_18:1_18:1)
TG(15:0_16:0_18:1)
TG(16:0_17:0_18:1)
TG(18:0_18:0_18:1)
TG(12:0_12:0_18:2)
TG(16:0_18:0_20:0)
TG(16:0_18:0_22:0) & TG(16:0_16:0_24:0)
TG(12:0_14:0_18:1) & TG(12:0_16:0_16:1)
TG(14:0_16:0_18:2)
TG(12:0_12:0_18:1)
TG(12:0_14:0_18:2) & TG(10:0_16:0_18:2)
TG(10:0_12:0_18:1)
TG(12:0_14:0_16:0)
TG(12:0_12:0_16:0)
TG(12:0_16:0_18:1) & TG(14:0_14:0_18:1)
TG(16:0_18:0_18:0)
TG(12:0_16:0_16:0)
TG(16:0_16:0_17:0) & TG(15:0_16:0_18:0)
TG(16:0_18:3_18:3)
TG(14:0_16:0_18:1)
TG(16:0_18:0_18:1)
TG(18:1_18:3_22:1)
TG(17:0_18:2_18:2) & TG(17:1_18:1_18:2)
TG(18:1_18:1_20:1)
TG(17:0_18:1_18:2)
TG(18:1_18:1_19:1)
TG(16:1_17:1_18:2) & TG(15:0_18:2_18:2)
TG(14:0_18:1_18:2) & TG(16:0_16:1_18:2)
TG(10:0_18:2_18:2)
TG(14:0_17:1_18:2) & TG(15:0_16:1_18:2)
TG(16:0_16:1_18:1) & TG(16:0_16:0_18:2)
TG(16:0_17:1_18:2) & TG(15:0_18:1_18:2)
TG(12:0_18:2_18:2)
TG(12:0_18:1_18:2)
TG(12:0_16:0_18:2)
TG(12:0_16:1_18:2)
TG(18:0_22:0_22:1) & TG(16:0_22:0_24:1)
TG(18:0_18:1_24:1)
TG(16:0_18:1_23:0)
TG(18:1_20:1_22:1) & TG(18:1_18:1_24:1)
TG(18:1_22:0_22:1) & TG(16:0_22:1_24:1)
TG(18:1_18:1_22:1)
TG(16:0_18:1_24:1) & TG(18:0_18:1_22:1)
TG(18:0_18:1_24:0)
TG(18:0_18:1_22:0) & TG(16:0_18:1_24:0)
TG(18:0_18:1_19:1)
TG(16:0_18:1_22:1) & TG(18:0_18:1_20:1)
TG(16:0_18:0_22:1) & TG(16:0_16:0_24:1)
LS3 LS1 LS2 KD1 KD2 KD3
f
1.5 1 0.5 0 -0.5 -1 -1.5
PC(20:4_20:4)
PC(p-40:6) / PC(o-40:7)A
PC(p-36:5) / PC(o-36:6)
PC(18:3_18:3)
PC(p-38:6) / PC(o-38:7)
PC(16:0_22:5)B
PC(16:0_16:0)
PC 42:10
PC(18:2_18:2)
PC(16:0_20:4)
PC(p-40:3) / PC(o-40:4)
PC(16:0_18:2)
PC(18:0_22:5)B
PC(18:0_22:6)
PC(18:1_20:5)
PC(p-38:3) / PC(o-38:4)B
PC(14:0_14:0)
PC(p-40:6) / PC(o-40:7)B
PC 37:4
PC(18:1_20:3)
PC(18:0_20:4)
PC 31:1
PC(14:0_16:0)
PC 31:0
PC 38:1
PC(p-32:1) / PC(o-32:2)
PC(18:1_18:1)
PC(18:1_18:2)
PC(16:0_20:3)
PC(18:2_18:3)B
PC 30:1
PC(18:0_18:1)
PC(18:0_20:3)
PC(16:0_18:3)a
PC(p-40:5) / PC(o-40:6)
PC 37:5
PC(p-38:3) / PC(o-38:4)A
PC(16:0_16:1)
PC(18:0_22:5)A
PC(16:0_18:1)
PC(20:0_18:2)
PC(18:2_20:4)
PC(16:0_22:6)
PC(14:0_20:4)
PC(p-38:5) / PC(o-38:6)A
PC(p-36:1) / PC(o-36:2)A
PC(p-34:0) / PC(o-34:1)
PC(p-38:4) / PC(o-38:5)A
PC(14:0_18:2)
PC(p-36:4) / PC(o-36:5)
PC(p-34:1) / PC(o-34:2)
PC(p-34:2) / PC(o-34:3)
PC 37:6
PC(p-42:5) / PC(o-42:6)A
PC(16:0_22:4)
PC(16:1_18:2)
PC(16:0_18:3)b
15:0-18:1(d7)PC
PC(18:2_22:5)
PC(18:2_18:3)A
PC(18:1_20:4)
PC(16:0_22:5)
PC(p-38:4) / PC(o-38:5)B
PC(16:1_22:6)
PC 42:8
LS3 LS1 LS2 KD1 KD2 KD3
g
Area Under the Curve
4×10^6
3×10^6
2×10^6
1×10^6
0
SC
KD

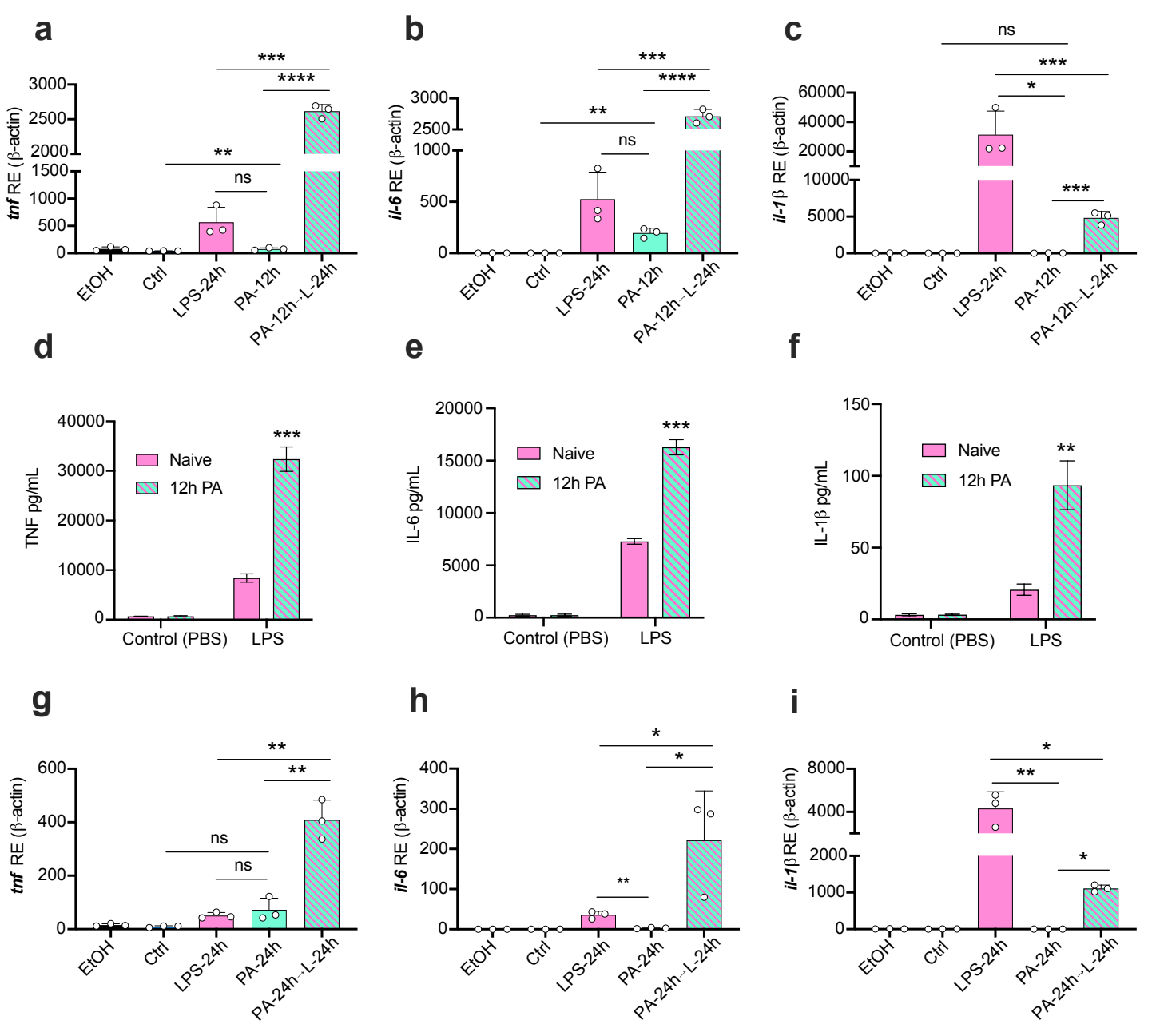
a
tnf RE (β-actin)
3000
2500
2000
1500
1000
500
0
***
****
**
ns
EtOH
Ctrl
LPS-24h
PA-12h
PA-12h→L-24h
b
il-6 RE (β-actin)
3000
2500
1000
500
0
***
****
**
ns
EtOH
Ctrl
LPS-24h
PA-12h
PA-12h→L-24h
c
il-1β RE (β-actin)
60000
40000
20000
10000
5000
0
ns
***
*
***
EtOH
Ctrl
LPS-24h
PA-12h
PA-12h→L-24h
d
TNF pg/mL
40000
30000
20000
10000
0
Naive
12h PA
***
Control (PBS)
LPS
e
IL-6 pg/mL
20000
15000
10000
5000
0
Naive
12h PA
***
Control (PBS)
LPS
f
IL-1β pg/mL
150
100
50
0
Naive
12h PA
**
Control (PBS)
LPS
g
tnf RE (β-actin)
600
400
200
0
**
**
ns
ns
EtOH
Ctrl
LPS-24h
PA-24h
PA-24h→L-24h
h
il-6 RE (β-actin)
400
300
200
100
0
*
*
**
EtOH
Ctrl
LPS-24h
PA-24h
PA-24h→L-24h
i
il-1β RE (β-actin)
8000
4000
2000
1000
0
*
**
*
EtOH
Ctrl
LPS-24h
PA-24h
PA-24h→L-24h

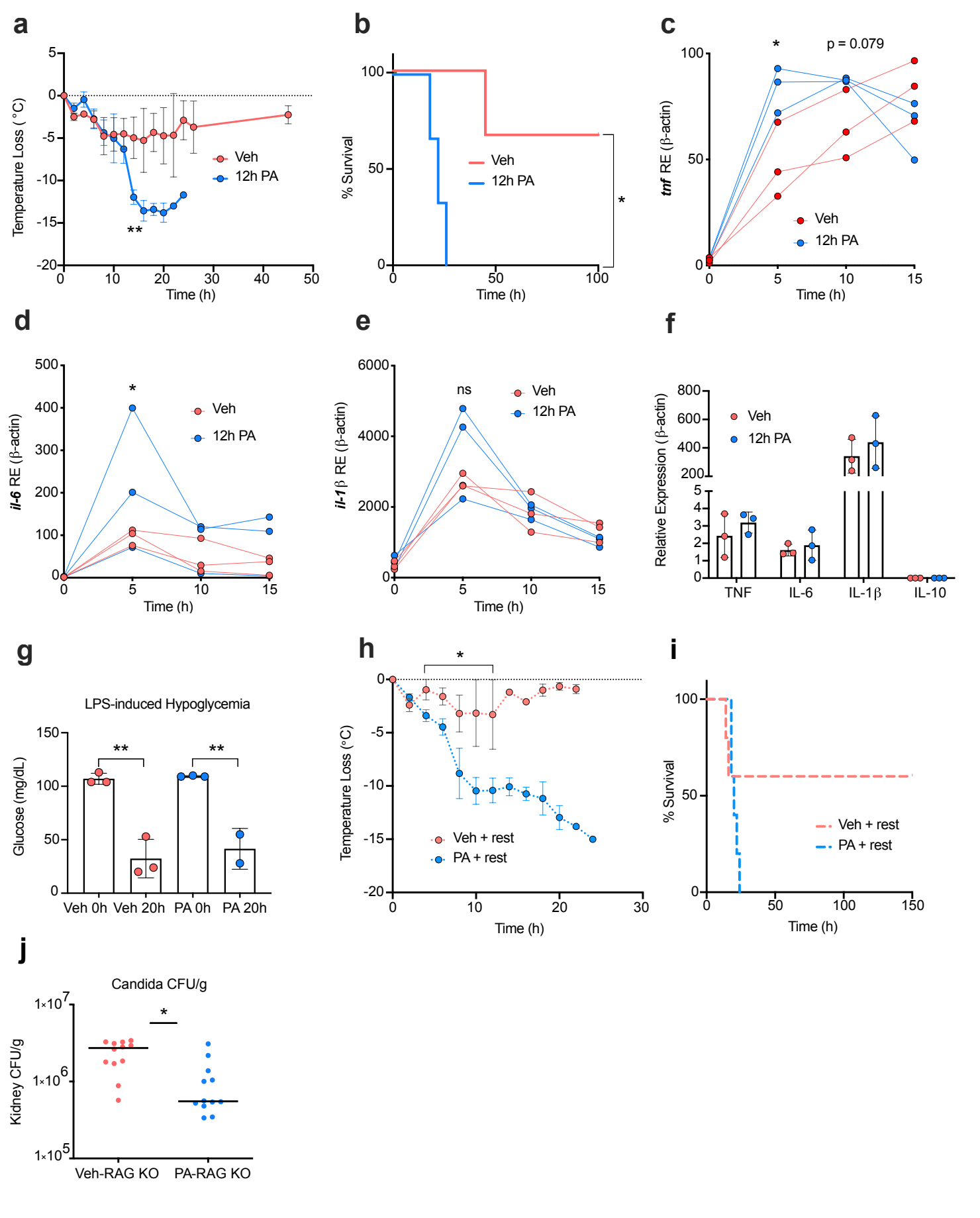
a
Temperature Loss (°C)
Time (h)
Veh
12h PA
**
b
% Survival
Time (h)
Veh
12h PA
*
c
tnf RE (β-actin)
Time (h)
*
p = 0.079
Veh
12h PA
d
il-6 RE (β-actin)
Time (h)
*
Veh
12h PA
e
il-1β RE (β-actin)
Time (h)
ns
Veh
12h PA
f
Relative Expression (β-actin)
Veh
12h PA
TNF
IL-6
IL-1β
IL-10
g
LPS-induced Hypoglycemia
Glucose (mg/dL)
**
**
Veh 0h
Veh 20h
PA 0h
PA 20h
h
Temperature Loss (°C)
Time (h)
*
Veh + rest
PA + rest
i
% Survival
Time (h)
Veh + rest
PA + rest
j
Candida CFU/g
Kidney CFU/g
*
Veh-RAG KO
PA-RAG KO